Bottling Liquid-Like Minerals for Advanced Materials Synthesis

Maxim B. Gindele, Sina Nolte, Katharina M. Stock, Kristina Kebel, and Denis Gebauer*

Materials synthesis via liquid-like mineral precursors has been studied since their discovery almost 25 years ago, because their properties offer several advantages, for example, the ability to infiltrate small pores, the production of non-equilibrium crystal morphologies or mimicking textures from biominerals, resulting in a vast range of possible applications. However, the potential of liquid-like precursors has never been fully tapped, and they have received limited attention in the materials chemistry community, largely due to the lack of efficient and scalable synthesis protocols. Herein, the "scalable controlled synthesis and utilization of liquid-like precursors for technological applications" (SCULPT) method is presented, allowing the isolation of the precursor phase on a gram scale, and its advantage in the synthesis of crystalline calcium carbonate materials and respective applications is demonstrated. The effects of different organic and inorganic additives, such as magnesium ions and concrete superplasticizers, on the stability of the precursor are investigated and allow optimizing the process for specific demands. The presented method is easily scalable and therefore allows synthesizing and utilizing the precursor on large scales. Thus, it can be employed for mineral formation during restoration and conservation applications but can also open up pathways toward calcium carbonate-based, CO_2-neutral cements.

1. Introduction

In the last decades, the effects of global climate change have become evident, for example, by an increasing rate of large-scale forest fires and droughts. There is consensus that climate change is mainly caused by anthropogenic emissions of greenhouse gases, while CO_2 is considered to be the main contributor to global warming.[1] In recent years, finding approaches to reduce anthropogenic CO_2 emissions has therefore been a key strategy in fighting climate change.[2] Besides the energy production and transportation sectors, industry is one of the main sources of global CO_2 emissions.[1,3] Especially the cement manufacturing process makes a significant contribution,[4] with some estimates attributing up to 10% of global CO_2 emissions to cement production.[5] Portland cement is one of the main components of concrete, the most widely used material on the planet, and improving cement sustainability is therefore a possible key towards reducing global CO_2 emissions.[6] Among a wide range of different approaches toward low-CO_2 cements,[5] one strategy is utilizing alternative materials for cement production, such as calcium carbonate-based cements, especially when combined with carbon capture and storage (CCS) technologies.[7] In comparison with other alternatives, calcium carbonate cements can be produced without decarbonization, thereby eliminating the main source of CO_2 during the cement manufacturing process.[8] Calcium carbonate cements have already been investigated with regard to their promising properties for biomedical applications.[9,10] Common methods for the synthesis of calcium carbonate cements are based on mixing solid amorphous calcium carbonates (ACC) with crystalline ones. Due to the lack of crystallization control during the cementation process, however, the resulting cements are microporous, show poor mechanical properties[9] and due to the difficulty in stabilizing the amorphous phase, are difficult to synthesize on an industrial scale.[11]

One promising solution to overcome these limitations of carbonate-based cementitious materials is, in our opinion, the polymer-induced liquid-precursor (PILP) process, an alternative crystallization pathway discovered by Laurie Gower in the late 1990s.[12,13] A PILP phase is essentially a polymer stabilized, highly hydrated amorphous mineral precursor phase that, due to the high water content, possesses a viscoelastic (often also referred to as "liquid-like") consistency. This viscoelastic consistency can be used to "mold" crystal structures via a so-called colloid assembly and transformation (CAT) process.[14–16] In this process, the liquid-like mineral droplets (colloids) can coalesce, thereby forming non-equilibrium structures, followed by a pseudomorphic amorphous-to-crystalline transformation, yielding crystalline minerals. In addition, the liquid-like properties allow the mineral precursor to infiltrate small cracks and pores, which is useful not only for the synthesis of biomimetic

M. B. Gindele, S. Nolte, K. M. Stock, K. Kebel, D. Gebauer
Institute of Inorganic Chemistry
Leibniz University Hannover
Callinstr. 9, D-30167 Hannover, Germany
E-mail: gebauer@acc.uni-hannover.de

materials,[15,17] but also for stone restoration and conservation applications, where infiltration and penetration of cracks and pores is favorable.[18] In the following, we will use the term "liquid-like precursor" to describe the highly-hydrated polymer-stabilized viscoelastic amorphous mineral precursor phase.

For essentially any commercially viable and practical application, easy, cheap, and large-scale synthesis of the liquid-like precursor phase is required. Until today, the synthesis is mostly based upon so-called gas-diffusion techniques, where CO_2 is released by a carbonate source, commonly ammonium carbonate, followed by diffusion of CO_2 and NH_3 into a solution of calcium ions and small amounts of polycarboxylates, usually poly(aspartic acid) or poly(acrylic acid).[12,19] After sufficient in-diffusion of CO_2, the mineral precursor precipitates in the form of micron sized droplets, yielding a few mg of product after several hours of reaction time.[20] Another possibility is the slow mixing of a dilute solution containing calcium ions with polycarboxylate and (bi)carbonate solution. In this case, it will also take several weeks to yield product even on a mg scale.[21] The dilemma of either synthesis strategy is that it is impossible to simply increase the concentrations of the solutions, as this would result in immediate precipitation of crystalline calcium carbonate (if Ca^{2+} and CO_3^{2-} concentrations are too high relative to the polymer concentration)[16] or of Ca-polymer coacervates (if Ca^{2+} and polymer concentrations are too high relative to the carbonate concentration).[22] Even if close attention is paid to avoid the precipitation of Ca-polymer coacervate phases, there is the risk of forming solid and unreactive ACC-polymer composite materials if the concentrations used are too high.[23–25] These composite materials do not possess liquid-like properties and also do not transform into the crystalline minerals due to their high polymer contents. A different strategy for mineral synthesis was recently demonstrated based on fluid-like ionic oligomer precursors[26] that possess similar advantages as the liquid-like precursors presented in this work, though their amount is limited due to the low solubility of salts in the employed ethanolic solutions. It is thus evident that the previously used synthesis methods are of highly limited practical use, as only small amounts of minerals can be synthesized. Also, the reaction times for liquid-precursor production via available synthesis methods take days (gas-diffusion) or weeks (mixing of dilute solutions), rendering the isolation of the precursor species prior to crystallization challenging. This has further hindered the utilization of liquid-like mineral phases in technological applications.[21,27] Due to the above-mentioned limitations of the available synthesis methods, the full potential of liquid-like mineral precursors in material synthesis has remained largely untapped in the past 25 years since their discovery.

We present an approach to synthesize liquid-like mineral precursors that uses highly concentrated starting solutions, thereby overcoming the limitations of previously known synthesis methods. We named the process "scalable controlled synthesis and utilization of liquid-like precursors for technological applications" (SCULPT). The SCULPT method allows scalable production of liquid-like mineral precursor, for example, using an automated titration essay,[28] which can then be isolated, their properties be optimized, and then be used for material synthesis based on the CAT process. In SCULPT, the concentrations of all species in the reaction solution can be precisely controlled by tuning starting concentrations and addition speeds. In this way, precipitation of side products, such as crystalline $CaCO_3$, Ca^{2+}-polymer coacervates or ACC-polymer composite materials is prevented, and a concentrated dispersion of the liquid-like mineral precursor is obtained. As the method is based on mixing of solutions in appropriate ratios, it can in principle be upscaled to an industrial, that is, multi-ton, scale, if appropriate equipment is used. In addition, the method can in theory also work with using CO_2 gas as carbonate source, which makes SCULPT interesting for CCS technologies. The product can be isolated by centrifugation and bottled or directly be applied to different substrates followed by controlled transformation of the precursor to yield the respective crystalline minerals. Additional additives, such as superplasticizers or metal ions, can be added during the synthesis to further tune the stability and properties of the precursor phase. The method yields several grams of liquid-like mineral precursor within a few hours, with the product then being stable against crystallization for several hours up to days depending on, for example, polymer molecular weight and Mg^{2+} content, allowing for the utilization of the unique viscoelastic properties of the precursor for different applications. Not only does this allow, for the first time, isolating the liquid-like precursor phase prior to crystallization, but also working with the precursor phase in application-relevant amounts as well as testing its performance in material synthesis, for example, in the formation of "molded" crystalline minerals and mineral coatings. Additional advantages of SCULPT are the easy in situ investigation and quantification of experimental conditions using potentiometric electrodes, such as pH value and free ion concentrations, and quantifying the effect of additives on the stability of the precursor phase. In our view, SCULPT significantly extends the toolbox of mineral synthesis approaches and will help overcoming practical problems in mineral synthesis, from built heritage conservation to CO_2-fixating cementitious materials.

2. SCULPT

SCULPT is based on an automated titration setup to simultaneously mix concentrated solutions of $CaCl_2$, Na_2CO_3, poly(acrylic acid) (PAA), and NaOH (**Figure 1**a) in a specific and controlled manner. The special procedure allows using much higher concentrations than previously, avoiding any side reactions, and was optimized as shown in Figure S1, Supporting Information. Thereby, all reactants are separated at the beginning of the experiment and are mixed directly in the reaction vessel in appropriate ratios, which prevents the precipitation of side products. In addition, the use of potentiometric electrodes allows the in situ detection of parameters such as pH value and calcium activities, enabling to quantify properties such as the solubility product of the formed mineral phases. Furthermore, it is possible to determine the point of crystallization of the precursor phase, allowing to estimate its kinetic stability. The ratios of added Ca^{2+}, CO_3^{2-}, and PAA are similar to previous liquid-like precursor syntheses,[12] however, SCULPT allows using up to 3 orders of magnitude higher concentrations. Solutions are added under vigorous stirring at rather slow rates (0.1 mL min^{-1}), preventing the formation of concentration gradients. After 6 h of reaction time the reaction vessel is filled up (Figure 1b) and the synthesis is complete. During the addition of the solutions, the calcium ion selective electrode (ISE) allows determining the activity of calcium

**ADVANCED
SCIENCE NEWS**

www.advancedsciencenews.com

**ADVANCED
MATERIALS**

www.advmat.de
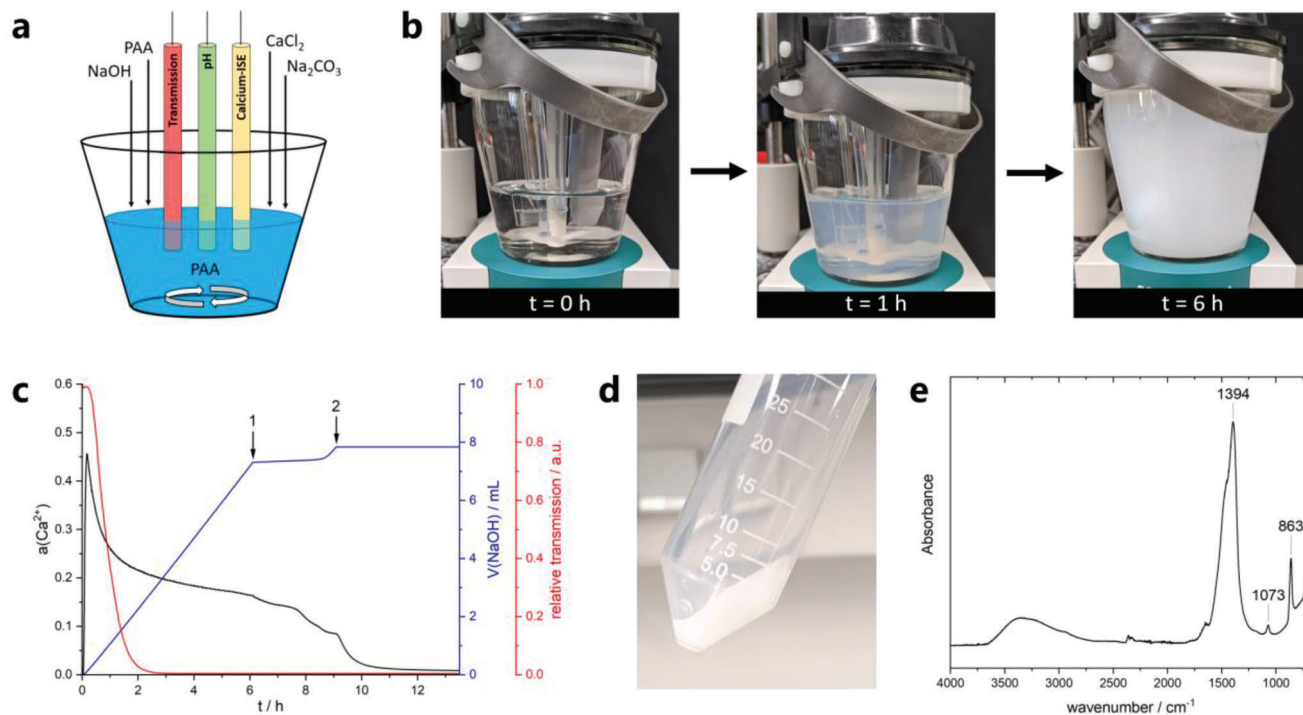
Figure 1. Synthesis of liquid-like mineral precursor. A) Scheme of the automated titration setup for SCULPT. Concentrated solutions of CaCl$_2$ (0.5 м), Na$_2$CO$_3$ (0.75 м), and PAA (10 g L^{-1}) are added at a constant rate (0.1 mL min^{-1}) into dilute PAA solution (1 g L^{-1}) under vigorous stirring, while the pH is kept constant at pH 10.65 by automatic addition of NaOH (0.5 м). Parameters such as pH, Ca^{2+} activity and transmission of the solution are recorded by potentiometric electrodes. B) Visual changes during the addition of the solutions. After 1 h, a visibly turbid dispersion is formed and after 6 h, when the reaction vessel is filled up, the dispersion is highly turbid. C) Data recorded by potentiometric electrodes during the addition of the solutions. The transmission of the solution/dispersion (red), Ca^{2+} activity (black), and volume of added NaOH solution so as to maintain a constant pH value (blue) are shown. After 6 h (point 1), the beaker is filled up and the addition of the solutions is stopped. The reaction can be further tracked, and crystallization is evident by a decrease in Ca^{2+} activity and an increase in NaOH addition (point 2). D) After the addition is finished (point 1 in c), the product can be isolated by centrifugation, resulting in several grams of a highly viscous dispersion of dense liquid precursor droplets. E) ATR-FTIR spectroscopy of the dried product. The broad ν_2 vibration at 863 cm^{-1} confirms the formation of ACC.[33] The detailed conditions for the experiments are listed in Table S1, Supporting Information.

ions in the solution, which, after phase separation, is governed by the solubility product of the most soluble solid phase present in the system. Indeed, phase separation occurs upon the drop in the calcium activity after reaching a maximum in the very beginning of the SCULPT experiment. The formed phase is characterized by a comparatively high calcium activity and is stable for several hours (Figure 1c, black curve), however, without reaching a constant value, that is, establishment of a solubility threshold. From quantitative evaluation of the measured calcium potential, the equilibrium ion activity product of the liquid–liquid coexistence in the mother solution can be estimated (Figure S2, Supporting Information), revealing much higher values than reported for solubilities of crystalline or (solid) amorphous calcium carbonates.[29,30] This is expected for an amorphous liquid-like precursor.[31] Upon crystallization of the amorphous precursor, a drop in the calcium potential is visible due to the formation of the more stable solid phase, even though quantitative data suggests that small amounts of the most soluble form of solid ACC persist (Figure S2, Supporting Information).[29] The crystallization point is also detectable via an increase in the NaOH addition rate, required to maintain a constant pH, due to the larger amount of carbonate ions bound from the buffer equilibrium upon crystallization (Figure S1, Supporting Information). During the addition

of the solutions in the SCULPT method, no sudden increase of NaOH addition occurs, corroborating that the precursor is amorphous (Figure 1c, blue curve). The amorphous character of the precursor was further confirmed by isolating species along the titration followed by characterization using attenuated-total reflection FTIR (ATR-FTIR) spectroscopy (Figure S3, Supporting Information), which clearly reveals the difference to previously reported ACC-PAA composite materials ("mineral plastics").[24] In parallel to the addition of the reactant solutions, the turbidity of the solution was measured and showed a rapid decrease during the first 3 h of the experiment (Figure 1c, red curve) due to the formation of a visibly turbid dispersion (Figure 1b). This is caused by the formation and growth of mineral precursor droplets of several µm in size, according to light microscopy (Figure S4, Supporting Information). After the reaction vessel is filled up (roughly after 6 h, Point 1 in Figure 1c), the resulting product can be isolated by centrifugation to obtain a highly concentrated dispersion of precursor droplets, possessing a gel-like consistency (Figure 1d). Interestingly, the product appears to be highly viscous directly after centrifugation but liquifies after manipulation with a spatula (Movie S1, Supporting Information). In total, 10–15 g of product can be isolated from one experiment on lab scale (using a 150 mL beaker). After liquifying, the
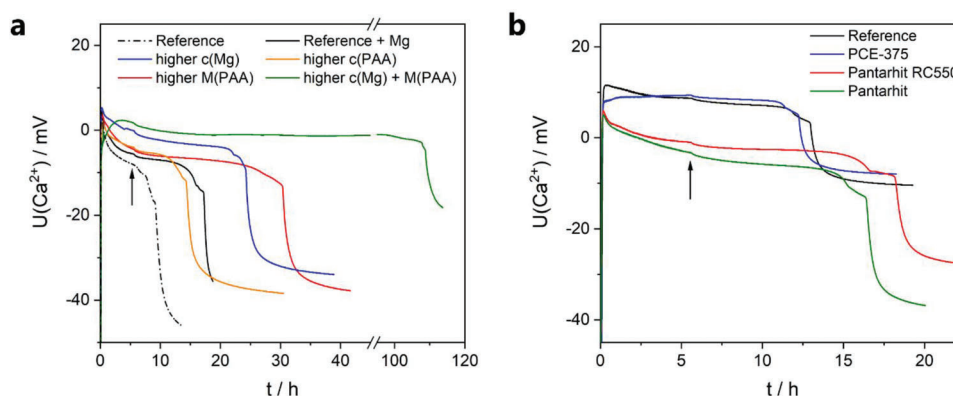
Figure 2. Effects of additives on the stability of mineral precursor. A) Titration curves for different ratios of Mg^{2+} and PAA concentrations in the added solutions. The reference conditions are shown in Figure 1c, using 10 g L^{-1} PAA with $M = 5000$ g mol^{-1} in the added solution. Conditions for the shown curves are as follows: Reference + Mg: addition of 25 mM Mg^{2+} (5 mol%) to the Ca^{2+} solution; higher c(Mg): 50 mM Mg^{2+} / 5 g L^{-1} PAA; higher c(PAA): 12.5 mM Mg^{2+} / 20 g L^{-1} PAA; higher M(PAA): 25 mM Mg^{2+} / 10 g L^{-1} PAA with $M = 100\,000$ g mol^{-1}; higher c(Mg) + M(PAA): 50 mM Mg^{2+} / 5 g L^{-1} PAA with $M = 100\,000$ g mol^{-1}. B) Titration curves for experiments with additional plasticizer in the starting solution. The initial concentration of plasticizer was 4 g L^{-1} in all experiments. Dosing of solutions was stopped at 6 h (arrow), and data was recorded until crystallization took place. Detailed conditions for titrations are shown in Table S1, Supporting Information.

product can be applied to substrates or filled in templates to produce minerals, as demonstrated below. If the product is dried in vacuum directly after centrifugation, amorphous calcium carbonate is obtained, as evident from the IR spectrum of the dried residue (Figure 1e). No polymer bands are visible in the IR spectrum, showing that the main product of the reaction is no Ca-PAA coacervate, but calcium carbonate mineral. The formation of Ca-PAA coacervates is a valid concern when high concentrations of Ca^{2+} and PAA are used,[32] and we indeed observe coacervate formation if no carbonate sources are used in the experiment. However, these Ca-PAA precipitates are vastly different from the liquid-like precursors formed in SCULPT (Figure S5, Supporting Information). Similarly, the formation of ACC-PAA composite materials as side products is of concern. If the concentrations of the polymer are significantly increased, we indeed observe the formation of a transparent ACC-polymer composite material with similar properties as other ACC inorganic-organic composites (Figure S6, Supporting Information).[23–25] However, these materials do not transform into crystalline calcium carbonates, even if suspended in water for extended periods of time and shall therefore not be discussed further. To conclude, at properly selected experimental conditions, SCULPT yields a concentrated dispersion of liquid-like mineral precursor droplets on a gram scale. The product is an initially amorphous dense liquid, and can be used to synthesize crystalline minerals, as shown below.

3. Effect of Additives

A key advantage of SCULPT is the quantification of the stability of the liquid-like precursor phase, that is, monitoring the time required until crystallization occurs. This is important as the precursor loses its liquid-like properties in the subsequent stages of mineralization when dehydration and crystallization take place. Therefore, there is a limited time for application in which the viscoelastic properties of the precursor phase can be exploited. To estimate this time for a given system, SCULPT can be used, but without isolating the product. In this case, except for the addition

of NaOH to keep the pH value constant, no further solutions are added, while stirring is continued and parameters are continuously recorded by the electrodes (Figure 1c). The crystallization of the precursor phase is then evident by a drop in the Ca^{2+} activity and an increase in the NaOH addition (Figure 1c, point 2, see also Figure S3, Supporting Information). This strategy is especially useful to investigate the effect of altered conditions, for example, changes in the concentrations of added solutions, or the effects of additives on the stability of the precursor phase.[28] At standard SCULPT reaction conditions (Figure 1), the precursor dispersion was stable for 2–3 h after the addition was stopped (Figure 1c, time between point 1 and 2). This stability is too low for most practical purposes, as only a few hours are available to apply the product until crystallization occurs and the advantageous liquid-like properties are lost. To solve this issue, additives can be used to increase the kinetic stability of the system. It is known that Mg^{2+} ions can stabilize ACC, especially if combined with polycarboxylates.[17,34,35] Therefore, $MgCl_2$ was added to the $CaCl_2$ solution, and the resulting effect on the stability of the precursor phase was explored. In addition, changes in PAA concentration were investigated (**Figure 2**a). It is evident that changes in the Mg^{2+} concentration have a larger effect than changes in the concentration of the polymer; with increasing Mg^{2+} concentration, we observe a strong increase in the kinetic stability of the precursor. Already the addition of 25 mM $MgCl_2$ to the $CaCl_2$ solution (corresponding to 5 mol% Mg^{2+} relative to the amount of Ca^{2+}) was sufficient to increase the precursor stability from 2 to 7 h, with 2 mol% Mg^{2+} being incorporated in the mineral after crystallization (Table S2, Supporting Information). Interestingly, this value is close to the Mg^{2+} content found in biominerals, such as sea urchin spines.[36] Using PAA with higher molecular weight ($M = 100\,000$ g mol^{-1}) also results in a strong stabilization. However, the viscosity of the product also increased drastically, and usually no liquification of the gel-like product (as shown in Movie S1, Supporting Information) was observed, hence compromising the liquid-like character. Therefore, although the stability of the precursor phase was lower, PAA with shorter chain

**ADVANCED
SCIENCE NEWS**

www.advancedsciencenews.com

**ADVANCED
MATERIALS**

www.advmat.de

length (M = 5000 g mol^{-1}) was used for further experiments. Thermogravimetric analysis (TGA) of the isolated, crystallized products shows that roughly 2–5 wt% of the polymer is present in the product (Table S2, Supporting Information). This reveals that in terms of practical applicability, changing conditions, and using additives affects not only the kinetic stability of the precursor phase, but the properties of the product during application and crystallization must be considered as well. Indeed, as already mentioned, the maximum kinetic stability can be reached when the concentrations of polymer are drastically increased, up to the point where no more crystallization takes place due to formation of ACC-PAA composite materials (Figure S6, Supporting Information). For the synthesis of liquid-like mineral precursor, it is, however, favorable to reduce the polymer content as much as possible, as polymers and other organic impurities can only be incorporated into crystalline CaCO$_3$ to a limited extend and will be excluded during the crystallization of the precursor phase (Figure S7, Supporting Information).[37,38] Exclusion of the polymer from the growing crystalline phase will result in the enrichment of the surrounding solution in polymer, which in turn will affect the efficiency of precursor fusion and crystallization.

Another difficulty in materials synthesis from liquid-like precursor is the formation of cracks during drying and crystallization of the precursor phase (Figure S6, Supporting Information) due to the high amount of water present. Therefore, as in the case of cement pastes, superplasticizer was added to the initial solution to reduce the water content while preserving workability of the product.[39] Several commercial plasticizers based on poly(carboxylate ether) or lignosulfonates were investigated with respect to their stabilizing efficiency and effect on the water content in the product (Figure 2b). Addition of polycarboxylate ether (PCE) plasticizers showed little effect on the stability of the precursor phase, while Pantarhit plasticizers caused a slight stabilization. However, the addition of PCE based plasticizer (concentration of 4 g L^{-1} in the initial solution) resulted in a reduction of the water content to 45% if multiple centrifugation steps were performed, which represents a significant improvement compared to plasticizer free products, that usually contain up to 80% water after centrifugation, independent of the number of centrifugation steps (Table S2, Supporting Information). Therefore, in addition to using 5 mol% Mg^{2+}, PCE based plasticizer was added to the titration experiments to synthesize an optimized precursor phase.

4. Material Synthesis from SCULPT Liquid-Like Mineral Precursor

Using the optimized reaction conditions, the application and material synthesis aspect was investigated. Again, it should be underscored that the SCULPT product is a highly concentrated dispersion of μm-sized amorphous mineral droplets in a salt-rich mother solution. As described earlier, the product can be directly dried to yield (solid) ACC, given that the time for drying is quicker than the time for crystallization of the precursor. However, starting from this ACC product, no large-scale minerals can be obtained due to the change in density from ACC (ρ = 1.62 g cm^{-3}) to calcite (ρ = 2.75 g cm^{-3}),[40] resulting in crack formation during transformation of ACC. Therefore, an advantageous strategy is to

let the assembly and crystallization of the precursor droplets happen directly in the solution (Figure S8, Supporting Information). Thereby, the droplets sediment and coalesce due to their liquid-like properties, resulting in the formation of larger mineral structures. In the same step, crystallization can take place yielding mineral structures without the problem of crack formation, as only small parts of the mineral crystallize at a time and potential ion-by-ion growth can fill interstitial spaces, similar to a recently reported growth mechanism for coral skeleton formation.[41] In addition, once crystallization has started, the growing crystalline structure can function as a substrate for further crystal growth, while polymer and plasticizer, which are not fully incorporated into the crystal (Figure S7, Supporting Information), are directly excluded and released into the mother solution at each step of crystallization. This way, formation of "pockets" of released additives are prevented and the formation of a solid mineral structure is possible. This strategy of crystallization in solution is in principle similar to the "conventional" gas diffusion-based synthesis of minerals using liquid-like precursors according to the CAT process.[15] Contrary to gas diffusion, however, in our experiments all droplets are present from the beginning, instead of being formed slowly during the gas diffusion process. While this is a much faster protocol for mineralization, one needs to pay attention to the stability of the droplets. If no coalescence takes place, the droplets will eventually dehydrate and crystallize in their dispersed state, losing their liquid-like properties. The following sedimentation will then lead to loose aggregates of crystalline CaCO$_3$ particles, which is evident by the difference in surface morphologies of mineral structures for increasing reaction times (Figure S9, Supporting Information). So as to obtain smooth mineral structures, the reaction has to be stopped before crystallization of the dispersed precursor droplets takes place. As described earlier, it is possible to estimate the stability of the precursor from the titration experiments, with the precursor usually being stable for several hours (Figure 2). After the desired reaction time, the remaining solution can be discarded and the product washed and dried, yielding the crystalline mineral (Figure S8, Supporting Information). Using this strategy, we demonstrate several possibilities for material synthesis from liquid-like precursors in the following.

One possibility is to use the precursor to synthesize mineral coatings on calcite crystals. The mineralization on top of existing mineral structures is relevant for applications in restoration and conservation, for example, in the restoration of marble structures. Small calcite crystals of several hundred μm in size were added to the precursor dispersions and mineralized. An even coating formed by the mineralized layer was visible in light microscopy (**Figure 3**a). Scanning electron microscopy (SEM) investigation of the surface shows that the layer was indeed formed by coalescence of precursor droplets, as still some semi-spherical features of individual droplets are visible (Figure 3b), while only minor cracks from drying occur on the surface. The observed mineral coatings look very similar to coatings formed by liquid-like precursors reported earlier,[21] which shows that our synthesis strategy can indeed produce results up to literature standard, with the ability to produce several orders of magnitude more of the precursor phase, in terms of quantity, rendering it practically usable in the first place. In several instances, SEM investigations of the dried specimens showed

**ADVANCED
SCIENCE NEWS**

www.advancedsciencenews.com

**ADVANCED
MATERIALS**

www.advmat.de
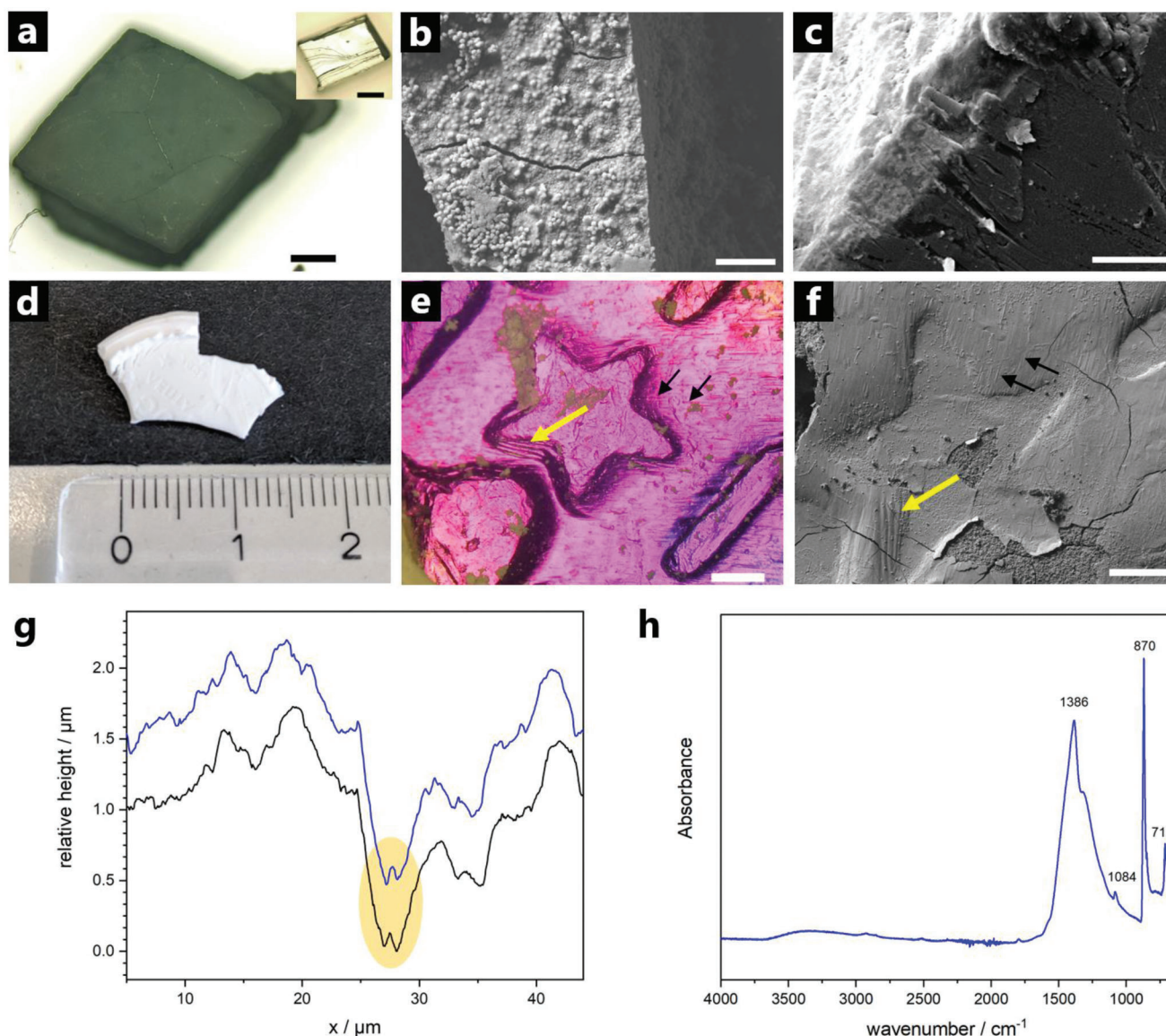
Figure 3. Application and material synthesis using liquid-like precursor. A) Calcite seed crystal covered with a layer mineralized from liquid SCULPT precursor. In the small inset, an uncovered calcite crystal is shown. Scale bars are 500 µm. B) SEM micrograph of a coating on a seed crystal formed by fusion of liquid-like precursor droplets. Scale bar is 10 µm. C) Cross section of a solid mineral layer formed on a calcite wafer. The layer shows even fusion of particles and a smooth surface. Scale bar 5 µm. D) Calcite mineral stamp of a coin with visible embossing. E) Light microscopy image of the surface of the coin after removing the molded mineral. Characteristic steps from the manufacturing process of the coin (yellow arrow) and scratches on the surface of the coin (black arrows) are highlighted. Scale bar is 250 µm. F) SEM micrograph of the mineral stamp, showing that the structures in from the coin shown in (e) are well reproduced. Scale bar 200 µm. G) Comparison of AFM line scans across a scratch on the coin and the corresponding imprint of the mineral mold. The yellow area highlights the resolution of a sample detail of a height of 80 nm. The shown lines are an average of $n = 10$ adjacent line scans across the sample. Raw data of the AFM scans is shown in Figure S15, Supporting Information. H) ATR-FTIR spectrum of the mineral mold. The characteristic vibrations at 870 and 712 cm^{-1} show the formation of calcite. Detailed conditions are summarized in Table S2, Supporting Information.

smooth structures formed by coalescence of the once liquid-like droplets (Figure S10, Supporting Information), which are similar to recently reported structures occurring in biomineralization involving liquid-like precursors.[42] Occasionally, solid mineral structures without involvement of seed crystals were observed (Figure S11, Supporting Information). In addition to seed crystals, we also used calcite wafers (5 × 5 mm in size) as template for the formation of mineral coatings. In these experiments,

the coatings deposited on the calcite templates usually showed a thickness of several µm, based on the use of 0.5 mL of precursor dispersion that was placed on top of the substrate (Figure 3c and Figure S9, Supporting Information). The mineralized layers were strongly attached to the seed crystal, and it was not possible to remove the layers from the substrate once deposited. In fact, treatment of the coated wafers using ultrasonication resulted in the substrate being damaged, while the mineralized layer

**ADVANCED
SCIENCE NEWS**

www.advancedsciencenews.com

**ADVANCED
MATERIALS**

www.advmat.de

remained attached (Figure S12, Supporting Information). These results demonstrate promising characteristics in using the precursor dispersion for mineral conservation and restoration applications, for which a strong adhesion of the mineralized layers is favorable.

The main advantage of using liquid-like precursors in the synthesis of minerals is their ability to infiltrate small pores or matrices, thereby enabling the production of structures that are inaccessible by conventional mineralization procedures. For example, commercial products for restauration of minerals are based on dispersions of calcium hydroxide particles of several hundreds of nm in size in ethanol.[43,44] It is easy to see that these conventional mineralization solutions based on (solid) particles are limited in their infiltration efficiency as soon as the dimensions of the template reach the dimensions of the particles, while a liquid, or liquid-like, precursor can easily "flow" into fine cracks. If we think of this "molding" of crystalline structures, the possible resolution and details should be much higher using a liquid-like precursor compared to (solid) particle-based approaches, which also will only produce an agglomeration of particles instead of an extended solid mineral structure. To demonstrate the use of liquid-like mineral precursors in these types of applications we placed the dispersion on a coin to test the efficacy of the precursor to infiltrate into the stamping and cracks on the surface of the coin. By letting the precursor droplets coalesce and crystallize, a "molded" mineral reflecting the features on the surface of the coin can be produced. In this way, molded minerals on a length scale of cm were produced (Figure 3d). Comparison of features embossed in the coin, for example, 1 mm sized stars (Figure 3e), with the produced mineral mold (Figure 3f) showed that the structure was well reproduced. In addition, details such as characteristic steps arising from the manufacturing process of the coin (Figure 3e,f, yellow arrows and Figure S13, Supporting Information) and even smaller scratches on the surface of the coin (Figure 3e,f, black arrows) were visible in the molded mineral material. The produced mineral stamp has a much higher resolution than achieved by the conventional mineral molding process using gypsum, which is limited to a scale of several tens of μm (Figure S14, Supporting Information). To estimate the resolution of our mineral cast, atomic force microscopy (AFM) was used to compare a scratch on the coin with its counterpart on the molded mineral (Figure S15, Supporting Information). Comparison of line scans across the scratch (Figure 3g) showed that features of <100 nm were resolved. Again, it needs to be mentioned that the investigated "molded" minerals are crystalline calcium carbonate, as revealed by the ATR-FTIR spectrum (Figure 3h). Thereby in all crystallization experiments calcite was formed as favorable crystalline polymorph. The manufacturing of crystalline minerals with the presented resolution visualizes the potential of material synthesis from liquid-like precursor phases, for example, regarding nanofabrication of minerals or new classes of mineral molding formulations with resolutions close to that of PDMS stamps.[45]

5. Conclusion

We have demonstrated a scalable experimental method to synthesize a liquid-like mineral precursor phase. The synthesis strategy solves the previously existing limitations of the available synthesis methods for liquid mineral precursors. Using the presented method, already on lab scale several grams of precursor phase with mineral contents of up to 50% can be synthesized within several hours, and SCULPT can be transferred to industrial scales in a straightforward manner. The titration-based method was also used to estimate the stability of the precursor and tune its stability by adding magnesium ions, while the workability of the product was improved by using superplasticizer. The liquid-like properties of the precursors synthesized using SCULPT can be used for material synthesis of different kinds of mineral materials with distinct applications, for example, the following:

i. Crystalline, solid $CaCO_3$ materials, having applications in restoration formulations,[46] and potential for use in calcium carbonate-based cements[7]
ii. "Molded" $CaCO_3$ minerals, having applications as high-resolution mineral molding formulation or for the synthesis of biomimetic materials[15,16,47]
iii. Crystalline $CaCO_3$ coatings with (or without) hierarchical ordering, having applications in soil-stabilization,[21] films for biomedical materials,[48] or coatings for oil-water separation[49]
iv. Polymer-ACC composite materials, having applications as sustainable "mineral" plastics,[24] protective packaging,[50] or glassy functional materials[25]
v. Polymer stabilized ACC materials or coatings, having applications as precursors for single crystals,[37,51] for inorganic monoliths[52] or for thin $CaCO_3$ films[53]
vi. Spherical calcite particles with narrow size distribution, having applications as filler or reinforcing materials[54] or drug delivery materials[55]

Our work enables the use of liquid-like precursor phases for material synthesis on application-relevant scales, possessing relevance for use in stone restoration, production of mineral molds, mineral coatings, as well as showing promise to produce mineral materials for construction chemistry, for example, toward the development and improvement of calcium carbonate based, CO_2-fixating cements.

6. Experimental Section

Materials: All solutions were prepared using Millipore water. Solutions of $CaCl_2$ and $MgCl_2$ were prepared by dissolution of $CaCl_2$ dihydrate (Sigma-Aldrich, ACS grade, >99%) and $MgCl_2$ hexahydrate (Sigma-Aldrich, ACS grade, >99%). NaOH solutions were prepared from NaOH stock solution (1.0 м, Carl Roth). Sodium carbonate solution was prepared by dissolution of Na_2CO_3 (Sigma-Aldrich, ACS grade, 99.95–100.05%). Poly(acrylic acid) (PAA) solution was prepared by dissolution of poly(acrylic acid) partial sodium salt (Aldrich, M = 5000 g mol^{-1} and M = 100 000 g mol^{-1}). Superplasticizers (FLUP PCE-375 by Backstein; Pantarhit RC550 and Pantarhit(FM) by Ha-Be Betonchemie), gypsum (MEYCO molding gypsum), and calcite crystals (optical calcite, Janine & Marc Köpke GbR) were purchased from commercial suppliers.

Synthesis of Mineral Precursor (SCULPT): A commercial automated titration setup (Metrohm Titrando) controlled by a computer software (Metrohm tiamo) was used. A titration device (905 Titrando) is controlling four dosing devices (800 Dosino) for the controlled addition of solutions of $CaCl_2$, NaOH, Na_2CO_3, and PAA, respectively. The calcium potential was monitored using a calcium ion selective electrode (Ca-ISE, Metrohm, No. 6.0508.110) and the pH was measured using a pH elec-

**ADVANCED
SCIENCE NEWS**

www.advancedsciencenews.com

**ADVANCED
MATERIALS**

www.advmat.de

trode (Metrohm, No. 6.0256.100). In addition, the transmission of the solution was measured with an Optrode (Metrohm, No. 6.1115.000) using a wavelength of 660 nm. The pH electrode was used as a reference electrode for the calcium electrode. The solution was stirred using an overhead stirrer (Metrohm, No. 2.802.0020). Calibration of the pH electrode was carried out at least twice per week using pH buffers from Mettler Toledo with pH 4.01 (No. 51 302 069), 7.00 (No. 51 302 047), and 9.21 (No. 51 302 070). The calcium ISE was calibrated by dosing 20 mм $CaCl_2$ solution with 0.01 mL min^{-1} into 50 mL Millipore water at the same pH value as the experiment.

In the following, the procedure for a standard precursor synthesis experiment is presented. The detailed conditions for all experiments discussed in the manuscript are summarized in Table S1, Supporting Information. Solutions of Na_2CO_3 (0.75 м), $CaCl_2/MgCl_2$ (0.5 м/0.025 м), and PAA (10 g L^{-1}) were added with rates of 0.1 mL min^{-1} into 50 mL of PAA solution (1 g L^{-1}) at pH 10.65. Prior to each experiment, the pH of this PAA starting solution was adjusted to pH 10.65 using 1 м NaOH. The experiments were performed in a sealed beaker under N_2 shower to prevent indiffusion of CO_2. During the experiment, the pH value was kept constant by automatic addition of 0.5 м NaOH, and the maximum possible stirring speed of the overhead stirrer (without introducing air bubbles) was used. The experiments were carried out for 6 h (33 mL of each solution added), before the vessel was full and the product was isolated. After each titration experiment, the beaker and electrodes were washed two times using acetic acid (10%, prepared by dissolution of glacial acetic acid) to remove traces of mineral precipitate from the vessel, electrodes, and dosing tips. Afterward, the equipment was rinsed several times with Millipore water and dried using dust-free tissue paper.

Isolation of Mineral Precursor: The mineral precursor was isolated by immediate centrifugation (15 min at 7000 *g*) after the titration was stopped. After discarding the mother solution, a gel-like, white precipitate was obtained that became a viscous liquid when it was stirred with a spatula. From one titration experiment, 10–15 g of concentrated mineral precursor dispersion were obtained. The product can directly be applied or be treated with an ultrasonic spear (Bandelin Sonopuls UW3100) for 2 min (at 20% power) to further reduce viscosity of the dispersion before application.

Mineralization Experiments: To produce mineral layers, 0.3 to 0.5 mL of the precursor dispersion were placed on a calcite single crystal wafer (5 × 5 mm). The wafers were stored in a closed petri dish to prevent evaporation of the solution. After the desired reaction time (usually several hours, check Table S2, Supporting Information for specific reaction times), the wafers were removed from the chamber, washed with Millipore water (to remove non-fused droplets) and dried on air for 1 d.

To produce mineral coatings on seed crystals, small calcite crystals (roughly 0.1–2 mm in size) were added directly to 5 mL of precursor dispersion in the centrifuge tube. The centrifuge tube was closed to prevent the dispersion from drying. After the desired reaction time, the particles were washed with water in an ultrasonic bath, the solution decanted and the crystals isolated by filtration, followed by drying on air for 1 day.

To produce mineral molds, 3–5 mL of the precursor dispersion were added on a regular German 50 ct coin. The coin was placed in a vessel with fitting diameter so that a layer of 0.5–1 cm of precursor dispersion was covering the coin. The vessel was covered with parafilm to prevent evaporation and left standing for 24 h. Then, the parafilm was removed and the dispersion slowly dried on air for 3 days. In some cases, the mineral mold separated from the coin in the drying step, while in other cases the mineral was removed from the coin using a spatula.

Material Characterization: Attenuated-total reflection Fourier-transform infrared (ATR-FTIR) spectra were recorded using a BRUKER Tensor 27 or Vertex 70v spectrometer. Scanning electron microscopy (SEM) and energy dispersive X-ray spectroscopy (EDX) was performed using a JEOL JSM-6610 SEM, while HR-SEM analysis (Figures S6d,e and S10, Supporting Information) was performed using a JEOL JSM-6700F SEM. Samples were coated with a 5–10 nm thick layer of gold (Cressington 108auto) prior to SEM analysis. Light microscopy images were recorded using a Keyence VHX-600 Digital Microscope equipped with a VHZ100UR Zoom Lens. Thermogravimetric analysis (TGA) was performed on a Netzsch STA 409 LUXX in O_2 atmosphere with a heating rate of 5 K min^{-1}. AFM was carried out on a Park Systems NX 10 microscope equipped with a PPP-NHCR cantilever in non-contact mode.

Statistical Analysis: All IR spectra were single recordings of the respective sample. For titration curves, usually several experiments were performed that showed very good reproducibility. For the sake of clarity, only a single, representative titration curve is shown in the figures.

Supporting Information

Supporting Information is available from the Wiley Online Library or from the author.

Conflict of Interest

M.G. and D.G. are inventors on a related and submitted patent application.

Data Availability Statement

The data that support the findings of this study are available from the corresponding author upon reasonable request.

[1] E. Benhelal, G. Zahedi, E. Shamsaei, A. Bahadori, *J. Cleaner Prod.* **2013**, *51*, 142.

[2] J. D. Figueroa, T. Fout, S. Plasynski, H. McIlvried, R. D. Srivastava, *Int. J. Greenhouse Gas Control* **2008**, *2*, 9.

[3] L. Huang, G. Krigsvoll, F. Johansen, Y. Liu, X. Zhang, *Renewable Sustainable Energy Rev.* **2018**, *81*, 1906.

[4] M. Schneider, M. Romer, M. Tschudin, H. Bolio, *Cem. Concr. Res.* **2011**, *41*, 642.

[5] U. Environment, K. L. Scrivener, V. M. John, E. M. Gartner, *Cem. Concr. Res.* **2018**, *114*, 2.

[6] E. Gartner, *Cem. Concr. Res.* **2004**, *34*, 1489.

[7] C. W. Hargis, I. A. Chen, M. Devenney, M. J. Fernandez, R. J. Gilliam, R. P. Thatcher, *Materials* **2021**, *14*, 2709.

[8] E. Gartner, in *Proceedings of the 31st Cement and Concrete Science Conference Novel Developments and Innovation in Cementitious Materials*, Imperial College London, London, UK, **2011**.

[9] C. Combes, B. Miao, R. Bareille, C. Rey, *Biomaterials* **2006**, *27*, 1945.

[10] M.-L. Fontaine, C. Combes, T. Sillam, G. Dechambre, C. Rey, in *New Calcium Carbonate-Based Cements for Bone Reconstruction*, Key Engineering Materials, Trans Tech Publications Ltd, Vol. 284, **2005**, pp. 105–108.

[11] D. Winters, K. Boakye, S. Simske, *Sustainability* **2022**, *14*, 4633.

[12] L. B. Gower, D. J. Odom, *J. Cryst. Growth* **2000**, *210*, 719.

[13] L. A. Gower, *The Influence of Polyaspartate Additive on the Growth and Morphology of Calcium Carbonate Crystals*, University of Massachusetts Amherst, **1997**.

[14] D. Gebauer, *Minerals* **2018**, *8*, 179.

[15] L. Gower, J. Elias, *J. Struct. Biol. X* **2022**, *6*, 100059.

[16] X. Cheng, L. B. Gower, *Biotechnol. Progr.* **2006**, *22*, 141.

[17] X. Cheng, P. L. Varona, M. J. Olszta, L. B. Gower, *J. Cryst. Growth* **2007**, *307*, 395.

[18] P. Ropret, K. Legan, K. Retko, T. Špec, A. Pondelak, L. Škrlep, A. S. Škapin, *J. Cult. Herit.* **2017**, *23*, 148.

[19] L. Gower, D. Tirrell, *J. Cryst. Growth* **1998**, *191*, 153.

[20] L. Dai, E. P. Douglas, L. B. Gower, *J. Non-Cryst. Solids* **2008**, *354*, 1845.

[21] C. Jenewein, C. Ruiz-Agudo, S. Wasman, L. Gower, H. Cölfen, *CrystEngComm* **2019**, *21*, 2273.

[22] S. Paris, D. Gruber, H. Cölfen, N. Bulgun, E. Prause, US 2022/0202657 A1, **2022**.

[23] D. Gebauer, V. Oliynyk, M. Salajkova, J. Sort, Q. Zhou, L. Bergström, G. Salazar-Alvarez, *Nanoscale* **2011**, *3*, 3563.

[24] S. Sun, L. B. Mao, Z. Lei, S. H. Yu, H. Cölfen, *Angew. Chem., Int. Ed.* **2016**, *55*, 11765.

[25] Y. Oaki, S. Kajiyama, T. Nishimura, H. Imai, T. Kato, *Adv. Mater.* **2008**, *20*, 3633.

[26] Z. Liu, C. Shao, B. Jin, Z. Zhang, Y. Zhao, X. Xu, R. Tang, *Nature* **2019**, *574*, 394.

[27] M. J. Olszta, D. J. Odom, E. P. Douglas, L. B. Gower, *Connect. Tissue Res.* **2009**, *44*, 326.

[28] A. Verch, D. Gebauer, M. Antonietti, H. Cölfen, *Phys. Chem. Chem. Phys.* **2011**, *13*, 16811.

[29] D. Gebauer, A. Völkel, H. Cölfen, *Science* **2008**, *322*, 1819.

[30] L. Brečević, A. E. Nielsen, *J. Cryst. Growth* **1989**, *98*, 504.

[31] J. T. Avaro, S. L. P. Wolf, K. Hauser, D. Gebauer, *Angew. Chem., Int. Ed.* **2020**, *59*, 6155.

[32] C. G. Sinn, R. Dimova, M. Antonietti, *Macromolecules* **2004**, *37*, 3444.

[33] L. Addadi, S. Raz, S. Weiner, *Adv. Mater.* **2003**, *15*, 959.

[34] S. L. Wolf, K. Jähme, D. Gebauer, *CrystEngComm* **2015**, *17*, 6857.

[35] D. Wang, A. F. Wallace, J. J. De Yoreo, P. M. Dove, *Proc. Natl. Acad. Sci. U. S. A.* **2009**, *106*, 21511.

[36] Y. Politi, R. A. Metzler, M. Abrecht, B. Gilbert, F. H. Wilt, I. Sagi, L. Addadi, S. Weiner, P. Gilbert, *Proc. Natl. Acad. Sci. U. S. A.* **2008**, *105*, 17362.

[37] J. Aizenberg, D. A. Muller, J. L. Grazul, D. Hamann, *Science* **2003**, *299*, 1205.

[38] L. Dai, X. Cheng, L. B. Gower, *Chem. Mater.* **2008**, *20*, 6917.

[39] F. Puertas, H. Santos, M. Palacios, S. Martínez-Ramírez, *Adv. Cem. Res.* **2005**, *17*, 77.

[40] J. Bolze, B. Peng, N. Dingenouts, P. Panine, T. Narayanan, M. Ballauff, *Langmuir* **2002**, *18*, 8364.

[41] C. Y. Sun, C. A. Stifler, R. V. Chopdekar, C. A. Schmidt, G. Parida, V. Schoeppler, B. I. Fordyce, J. H. Brau, T. Mass, S. Tambutte, P. Gilbert, *Proc. Natl. Acad. Sci. U. S. A.* **2020**, *117*, 30159.

[42] C. A. Stifler, C. E. Killian, P. U. Gilbert, *Cryst. Growth Des.* **2021**, *21*, 6635.

[43] C. Rodriguez-Navarro, A. Suzuki, E. Ruiz-Agudo, *Langmuir* **2013**, *29*, 11457.

[44] E. Tedesco, I. Mičetić, S. G. Ciappellano, C. Micheletti, M. Venturini, F. Benetti, *Toxicol. In Vitro* **2015**, *29*, 1736.

[45] B. D. Gates, Q. Xu, M. Stewart, D. Ryan, C. G. Willson, G. M. Whitesides, *Chem. Rev.* **2005**, *105*, 1171.

[46] C. Rodriguez-Navarro, K. Elert, R. Ševčík, *CrystEngComm* **2016**, *18*, 6594.

[47] L. B. Mao, Y. F. Meng, X. S. Meng, B. Yang, Y. L. Yang, Y. J. Lu, Z. Y. Yang, L. M. Shang, S. H. Yu, *J. Am. Chem. Soc.* **2022**, *144*, 18175.

[48] C. Xiao, M. Li, B. Wang, M.-F. Liu, C. Shao, H. Pan, Y. Lu, B.-B. Xu, S. Li, D. Zhan, *Nat. Commun.* **2017**, *8*, 1398.

[49] M. Li, Y. Chen, L. B. Mao, Y. Jiang, M. F. Liu, Q. Huang, Z. Yu, S. Wang, S. H. Yu, C. Lin, X. Y. Liu, H. Cölfen, *Langmuir* **2018**, *34*, 2942.

[50] T. Saito, Y. Oaki, T. Nishimura, A. Isogai, T. Kato, *Mater. Horiz.* **2014**, *1*, 321.

[51] S. Zhang, O. Nahi, X. He, L. Chen, Z. Aslam, N. Kapur, Y. Y. Kim, F. C. Meldrum, *Adv. Funct. Mater.* **2022**, *32*, 2207019.

[52] Z. Mu, K. Kong, K. Jiang, H. Dong, X. Xu, Z. Liu, R. Tang, *Science* **2021**, *372*, 1466.

[53] X. Xu, J. T. Han, K. Cho, *Chem. Mater.* **2004**, *16*, 1740.

[54] J. Yu, M. Lei, B. Cheng, *Mater. Chem. Phys.* **2004**, *88*, 1.

[55] Y. Boyjoo, V. K. Pareek, J. Liu, *J. Mater. Chem. A* **2014**, *2*, 14270.